EEG-Rhythm Specific Taylor-Fourier filter bank Implemented with O-splines for the Detection of Epilepsy using EEG Signals

Article *in* IEEE Sensors Journal · February 2020

DOI: 10.1109/JSEN.2020.2976519

5 authors, including:

Mario R Arrieta Paternina
National Autonomous University of Mexico (UNAM), Mexico City, Mexico

Alejandro Zamora-Mendez
Universidad Michoacana de San Nicolás de Hidalgo

RK Tripathy
BITS Pilani, Hyderabad

Ram Bilas Pachori
Indian Institute of Technology Indore

EEG-Rhythm Specific Taylor-Fourier filter bank Implemented with O-splines for the Detection of Epilepsy using EEG Signals

José Antonio de la O Serna, Mario R. Arrieta Paternina, Alejandro Zamora-Méndez, Rajesh Kumar Tripathy, and Ram Bilas Pachori

***Abstract*—The neurological disorder which is associated with the abnormal electrical activity generated from the brain causing seizures is typically termed as epilepsy. The automated detection and classification of epilepsy based on the analysis of the electroencephalogram (EEG) signal are highly required for its early diagnosis. In this paper, we have developed an EEG-rhythm specific Taylor-Fourier filter-bank implemented with O-splines for the detection and classification of epilepsy from the EEG signal. The energy features are evaluated from the Taylor-Fourier sub-band signals of the EEG signal. The classifiers such as K-nearest neighbor (KNN) and least square support vector machine (SVM) are employed for the classification of normal, seizure-free and seizure from the Taylor-Fourier EEG-band energy (TFEBE) features. The experimental results demonstrate that, for the classification of normal, seizure-free, and seizure classes, the least square SVM classifier has an overall accuracy value of 94.88% using the EEG signals from the Bonn university database. The proposed EEG rhythm specific Taylor-Fourier filter-bank with O-splines can be implemented in real-time for the detection of epileptic seizures from EEG signals.**

***Index Terms*—Seizure, Electroencephalogram , Taylor-Fourier Filter-bank, O-splines, Least-square SVM, Accuracy.**

I. INTRODUCTION

THE epilepsy is a neurological disease that affects nearly 50 million people in the entire world [1]. This neurological disorder is characterized by the re-occurrence of epileptic seizures [2]. The electroencephalogram (EEG) signals are commonly used for the diagnosis of epilepsy by the doctors and neurologists, whose generally perform diagnosis of epilepsy based on the visual inspection of the EEG signal, which is a time-consuming task and subjective in nature since these recordings are done for longer duration [3], [4]. Such reasons challenge to the researchers to develop automated methods using machine learning algorithms and signal processing techniques for the diagnosis of epilepsy from EEG signals [5] [6].

J. de la O is with the Department of Electrical Engineering, Autonomous University of Nuevo Leon, Monterrey, NL 66450, Mexico (e-mail: jdelao@ieee.org).

A. Zamora is with Electrical Engineering Faculty, Universidad Michoacana de San Nicolas de Hidalgo, Morelia, Mich. 58030, Mexico, (e-mail: azamoram@umich.mx).

M. R. A. Paternina is with the Department of Electrical Engineering, National Autonomous University of Mexico, Mexico City 04510, Mexico, (e-mail: mra.paternina@fi-b.unam.mx).

R. K. Tripathy is with the Department of Electrical and Electronics Engineering, BITS-Pilani, Hyderabad Campus, Hyderabad, 500078, India, (e-mail: rajeshiitg13@gmail.com).

Ram Bilas Pachori is with Discipline of Electrical Engineering, Indian Institute of Technology Indore, Indore-453552, India. e-mail: pachori@iiti.ac.in

The EEG signals are non-stationary signals or time-varying signals [7]. In the literature, a plethora of methods has investigated different signal processing techniques and machine learning algorithms for the automated detection of epileptic seizures using the EEG signals [8]. The method in [9] suggests the separation of rhythms of EEG signals based on the Fourier-Bessel series expansion (FBSE) and the extracted features from these rhythms have been used for the automatic classification of epileptic seizure EEG signals. The tunable Q wavelet transform (TQWT)-based method together with multi-scale entropy have been explored for automated detection of epileptic seizure EEG signals in [10]. In [11], the analytic time-frequency flexible wavelet transform has been studied for the automated classification of EEG signals. In [12], the features extracted from the time-frequency domain of EEG signal have been for the classification of epileptic seizures. These features have been evaluated using the improved eigenvalue decomposition of the Hankel matrix (IEDHM) and Hilbert transform (HT). The FBSE based empirical wavelet transform has been studied for automated classification of epileptic seizures from EEG signals in [13]. The research work presented in [10] has used the multi-scale radial basis functions (MRBF) and modified swarm optimization for the classification of seizure and seizure-free EEG signals. The Hilbert-Huang transform based tensor representation has been applied in [14] for non-convulsive seizure detection. In [15], the time-frequency images obtained from the EEG signals have been used for the epileptic seizure detection. The time-frequency localized three-band bi-orthogonal filter bank has been applied to EEG signals for epileptic seizure detection in [16]. The classification of seizure and seizure-free classes has been carried out based on the phase space representation of intrinsic mode functions of EEG signals in [17]. In [18], the fractional linear prediction (FLP) method has been used for the detection of epileptic seizures from EEG signals. The dual free complex wavelet transform method has been applied for the detection of epileptic seizures from EEG signals in [19]. The local neighbor descriptive pattern has been explored for the identification of epileptic seizures from the EEG signals in [20]. In [21], the time-frequency analysis and the time-varying autoregressive model have been explored for the automated detection of epileptic seizures from EEG signals. In [22], the authors have used time-frequency analysis and artificial neural network (ANN) for the automated classification of seizure and seizure-free categories from the EEG signals. The Hilbert-Huang transform (HHT) and support vector machine (SVM) have been studied for the automated identification of epileptic seizures from the EEG signals in [23]. In [24], the authors have proposed the wavelet-based fuzzy approximate entropy for the detection of epileptic seizures from EEG signals.

The above-reported methods have extracted various non-linear features in the time-domain or transformed domain of the EEG signal for the classification of epileptic seizures. The detection of epileptic seizures based on the new signal processing techniques is a challenging research domain in biomedical engineering. This paper introduces the Taylor-Fourier filter-bank designed with O-splines for the detection of epileptic seizures from EEG signals. The major advantages of the O-splines derived from the digital Taylor-Fourier subspace are enclosed in [25], being remarkable the reduction of the computational complexity due to only a selective number set of FIR filters is designed avoiding large computations to build the Taylor-Fourier matrix and its pseudo-inverse. This implementation overcomes the proposal in [26] providing filters with a wider frequency band, and with the ability to be adaptable according to the application. The main advantage of Taylor-Fourier transform is that the O-splines perform a uniform division of the spectrum [25]. The Taylor-Fourier filter-bank based analysis of the ECG signal has shown better performance for the detection of heart ailments [26]. It can be expected that the band specific Taylor-Fourier filter-bank based analysis will be effective for simultaneous separation of rhythms from the EEG signal and detection of the epileptic seizures. In this study, we have extracted energy features from the Taylor-Fourier sub-band signals of the EEG signal, and these extracted features are used into the least square SVM-based classifier to distinguish between seizure and seizure-free episodes. The remaining sections of this paper are structured as follows. In Section II, the proposed method is described. We have presented the results and the discussion of this paper in Section III. Then, the concluding remarks are drawn in the last section.

II. Method

The proposed method for the detection of epileptic seizures is outlined in Fig. 1, consisting of the collection of EEG signals from public database, design of the Taylor-Fourier with O-splines based filter-bank for the analysis of EEG signals, extraction of energy features from each sub-band signal and the classification is carried out by the least square SVM-driven classifier.

A. EEG database

In this investigation, the EEG signals from the Bonn University database [27] have been used to verify the effectiveness of the proposed method for the automated identification of epileptic seizures from EEG signals. This database includes recordings of EEG signals obtained from healthy subjects and epileptic patients and it is publicly available at [1]. This database has five subsets and each one has been denoted by Z, O, N, F, and S. In subsets Z and O, there are 100 recordings of the single-channel EEG signals. These recordings have been obtained from five healthy persons using surface electrodes. The N and F subsets include 100 recordings of the single-channel EEG signals in each subset which have been recorded from epileptic patients during seizure-free intervals. The subset S contains 100 recordings of single-channel EEG signals from the patients during the epilepsy attack. The EEG signals in subset F have been recorded during seizure-free intervals from five patients in the epileptic zone [27]. On the other hand, the subset N contains the recording of EEG signals from the hippocampal formation of the opposite hemisphere of the brain. The subsets Z and O contain on face EEG recordings whereas N, F, and S subsets contain intra-cranial EEG recordings. These subsets (Z, O, N, F, and S) contain 100 EEG signals in each, with a sampling rate of 173.61 Hz. In this research, we have classified normal, seizure, and seizure-free classes of EEG signals. These classes of EEG signals are obtained by combining subsets as follows: (Z, O), (S), and (N, F). Here, we have discussed the database in a brief manner. For more detailed information related to the database, please refers to the study in [27]. In this study, we have proposed the epileptic seizure detection method for patients with epilepsy and the normal subjects who never had epilepsy attacks. The proposed method can be used by the patients in order to detect epileptic seizures. On the other hand, normal people can also have an epilepsy attack and can be detected in an automated manner with the help of the proposed framework.

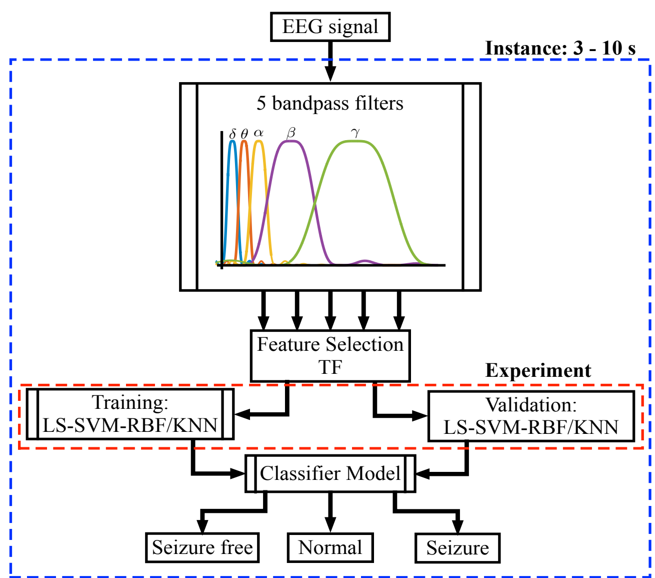

Fig. 1. Block-diagram of the proposed method for the detection of epileptic seizure from EEG signal.

B. Taylor-Fourier Filter Bank with O-Splines

The finite impulse response (FIR) filters used to analyze the EEG signal are designed with the basic ideas of the Discrete Taylor-Fourier transform (DTFT). In [25], the author has verified that the common envelopes of the DTFT filter impulse responses are referred to as O-splines. The O-splines are obtained numerically from the inverse of the Taylor-Fourier

[1] www.meb.unibonn.de/epileptologie/science/physik/eegdata

TABLE I
FREQUENCY SPECIFICATION OF DESIRED FILTERS [28].

Filter No.	F_{min}(Hz)	F_c (Hz)	F_{max} (Hz)
1	0	2	4
2	4	6	8
3	8	11	14
4	14	22	30
5	30	44	58

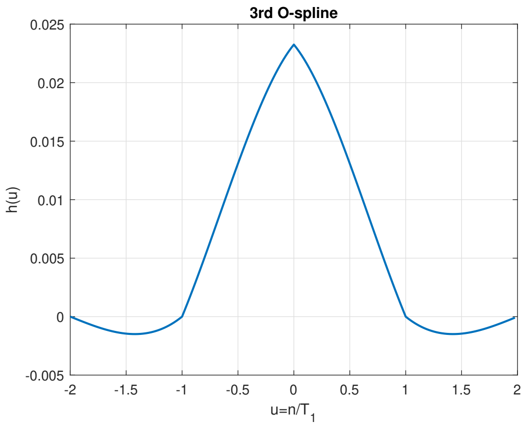

Fig. 2. Third O-spline as impulse response of the lowpass filter for the first two bandpass filters.

operator $\tilde{\Phi}$ [25]. The DTFT of an EEG signal, $z(n)$ can be written as follows [25]:

$$z(n) = \sum_{h=-H}^{H} \xi_h(n) e^{j2\pi h f_1 n}, \qquad -C\frac{N}{2} \leq n \leq C\frac{N}{2}, \quad (1)$$

where $n = 0, 1, ..., N-1$ are the samples of EEG signal and h is the harmonic and f_1 is the fundamental frequency. C is the number of cycles and is defined as $C = K + 1$, where K is the order of the Taylor polynomial. Similarly, $\xi_h(n)$ is the Taylor-Fourier coefficients of the h^{th} harmonic of the EEG signal. The bandlimited approximated dynamic harmonics are evaluated using the Taylor series expression as,

$$\xi_h^{(K)}(n) = \xi_h(n_0) + \dot{\xi}_h(n_0) + \cdots + \xi_h^{(K)}(n_0)\frac{n^K}{K!}, \qquad (2)$$

Thus, the EEG signal model for the K-th order extension is given as follows [29]:

$$\mathbf{z}_K = \Phi_K \xi_K$$
$$= \begin{pmatrix} I \begin{pmatrix} W_N \\ W_N \\ \vdots \\ W_N \end{pmatrix} & T \begin{pmatrix} W_N \\ W_N \\ \vdots \\ W_N \end{pmatrix} & \cdots & \frac{1}{K!}T^K \begin{pmatrix} W_N \\ W_N \\ \vdots \\ W_N \end{pmatrix} \end{pmatrix} \begin{pmatrix} \xi_N \\ \dot{\xi}_N \\ \vdots \\ \xi_N^{(K)} \end{pmatrix} \qquad (3)$$

where the $(K+1)N \times (K+1)N$ matrix Φ contains the basis vectors of the extended subspace, the subvector ξ_N contains the set of K-th degree Taylor-Fourier coefficients, the subvectors $\xi_N^{(k)}, k = 1, \ldots K$ their progressive derivatives, and N is the number of samples per fundamental cycle. In [25], the matrix Φ_K is factorized as follows:

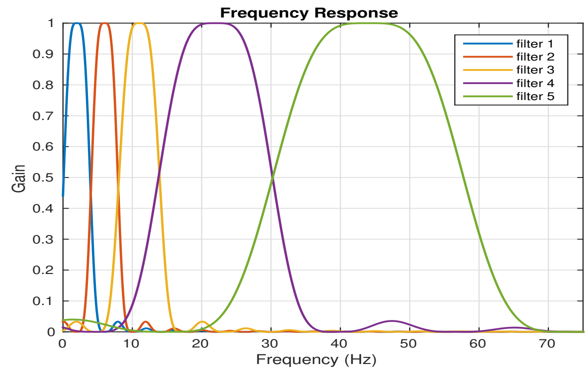

Fig. 3. Frequency response of the designed bandpass filters.

$$\Phi_K = \Upsilon_K \Omega_K$$
$$= \begin{pmatrix} I & T_1 & \cdots & \frac{1}{K!}T_1^K \\ I & T_2 & \cdots & \frac{1}{K!}T_2^K \\ \vdots & \vdots & \ddots & \vdots \\ I & T_C & \cdots & \frac{1}{K!}T_C^K \end{pmatrix} \begin{pmatrix} W_N & 0 & \cdots & 0 \\ 0 & W_N & \cdots & 0 \\ \vdots & \vdots & \ddots & \vdots \\ 0 & 0 & \cdots & W_N \end{pmatrix} \qquad (4)$$

where submatrices $T_i, i = 1, 2, \ldots, C$ are diagonal matrices including the segment of the K-th Taylor term. In this factorization, the Taylor-Fourier operator Φ_K is separated into two matrices: Υ for the Taylor operator, and Ω for the Fourier one. Its dual matrix $\tilde{\Phi}_K$ is found to be of the form (5). Notice its vectors are harmonic modulations of the vertical subdiagonals in $\tilde{\Upsilon}$, which contain the segments of the O-splines and its derivatives. These perform as envelopes of the bandpass filters at the harmonic frequencies of the DTFT.

$$\tilde{\Phi}_K = \Upsilon(\Upsilon^H \Upsilon)^{-1}\frac{\Omega}{N} = \tilde{\Upsilon}\frac{\Omega}{N} \qquad (5)$$

By implementing the O-splines and derivatives as lowpass filters the computational complexity of the DTFT is dramatically decreased, since it is reduced to a small number of finite impulse response (FIR) filters [25]. In this work, if we only need to extract the $\delta, \theta, \alpha, \beta, \gamma$ rhythms from the EEG signal then we need 5 FIR filters of $(K+1)N$ length per observed frequency.

Since the analysis of EEG signals requires filters with increasing bandwidths, their impulse responses will be obtained by time contraction of the used O-spline. The $3rd$ order O-spline is basically the envelope of the DTFT filters with $K = 3$. Here, it is obtained in closed form in the inverse matrix of the Taylor operator, and rearranging the elements of its vertical diagonal sub-matrices. We have:

$$\upsilon_0^{(3)}(u) = \begin{cases} \frac{1}{6}u^3 + u^2 + \frac{11}{6}u + 1 & \text{for } -2 \leq u < -1, \\ -\frac{1}{2}u^3 - u^2 + \frac{1}{2}u + 1 & \text{for } -1 \leq u < 0, \\ \frac{1}{2}u^3 - u^2 - \frac{1}{2}u + 1 & \text{for } \quad 0 \leq u < 1, \\ -\frac{1}{6}u^3 + u^2 - \frac{11}{6}u + 1 & \text{for } \quad 1 \leq u < 2, \\ 0 & \text{otherwise,} \end{cases} \qquad (6)$$

in which $u = n/T_1$, with $T_1 = 1/F_1$, and F_1 is the bandwidth of the desired filter. Since the O-spline is symmetric, only the first (or the last) two polynomials are needed to obtain the rest of the elements of the dual Taylor matrix. The following vectors of the dual matrix are obtained by recursive differentiation: $\upsilon_1^{(3)} = -F_1 \frac{\mathrm{d}}{\mathrm{d}u}\upsilon_0^{(3)}$, $\upsilon_2^{(3)} = -F_1 \frac{\mathrm{d}}{\mathrm{d}u}\upsilon_1^{(3)}$, and $\upsilon_3^{(3)} = -F_1 \frac{\mathrm{d}}{\mathrm{d}u}\upsilon_2^{(3)}$. The advantages of using O-splines for designing EEG rhythm specific Taylor-Fourier filter-bank are given as follows. The O-splines of the Taylor-Fourier filter bank provides the best coefficients (samples) in the analysis equation, and with the lowest error in the synthesis equation, with the shortest impulse response. Other bandpass filters could be used, but none of them will provide better results in the subspace spanned by the DTFT signal model, since the DTFT solution is unique in that subspace [25]. For the EEG analysis, five FIR filters are needed with the specifications in Table I, in which F_c is the central frequency and $[F_{min}, F_{max}]$ delimits the required passband. The sampling frequency of the available data is $F_s = 173.61$Hz with a sampling time T_s of 5.8 ms [27]. These frequency ranges are considered for the separation of rhythms using the Taylor-Fourier filter bank. It should be noted that the same filter parameters as mentioned in Table I have been used for the design of 5 band-pass filters in order to separate the rhythms of EEG signals corresponding normal, seizure-free, and seizure classes. Due to the synchronization of neural actives during seizure activity, the presence of spikes (impulsive nature) and higher amplitude take place in the corresponding EEG signals [30]. Due to these reasons, various frequency-bands corresponding to the rhythms together with their energy have been explored for determining features in order to correlate them with epileptic seizures. Fig. 2 shows the impulse response of the low-pass filter for the first two bandpass filters. It was designed using a bandwidth of $F_1 = 4$ Hz. In consequence, the number of samples per period T_1, is $N_1 = 43$. In a similar way, the last three bandpass filters were designed with $N_1 = 28, 10, 6$ respectively. In this study, the impulse responses for the EEG signal are denoted as $\mathbf{h}_1$, $\mathbf{h}_2$, $\mathbf{h}_3$, $\mathbf{h}_4$, and $\mathbf{h}_5$, respectively. Thus, $\mathbf{h}_i(u)$, for $i = 1, \dots, 5$ is expressed by (7)

$$\mathbf{h}_i(u) = [h_{i1}\ h_{i2}\ h_{i3}\ h_{i4}] * e^{jFc\theta_1/N_1} \tag{7}$$

where h_{i1}, h_{i2}, h_{i3}, h_{i4} are the rows of (6), Fc is given in Table I, $\theta_1 = 2\pi/F_s$, and $N_1 = 43, 28, 10, 6$, respectively for the five impulse responses. Fig. 3 shows the frequency response of the implemented filters.

The rhythms are obtained using the convolution (*) of EEG signal with impulse responses of the filters which are obtained using O-splines, $z_b(n) = s(n) * h_b$, where $b \in \{\delta, \theta, \alpha, \beta, \gamma\}$ corresponds to the EEG-band number ($h_i, i = 1, \dots, 5$, respectively in (7), and $s(n)$ are frames of the EEG signal. The EEG signals and the rhythms for normal, seizure-free and seizure classes are shown in Fig. 4. It is observed that the EEG signal characteristics are different for normal, seizure and seizure-free classes. The rhythms evaluated using the proposed filter-bank capture the variations of the EEG signal in its components or rhythms for each class. The features extracted from these rhythms can be used for the classification of seizure and seizure-free classes.

C. Feature Extraction and least square SVM-based Classifier

In this study, we have extracted the energy features from each rhythm of EEG signal and these features are denoted as TFEBE. The TFEBE features from the EEG-rhythms ($z_\delta(n)$, $z_\theta(n)$, $z_\alpha(n)$, $z_\beta(n)$, and $z_\gamma(n)$) are evaluated as

$$TFEBE_b = \sum_{n=1}^{N} |z_b(n)|^2 \tag{8}$$

where $b \in \{\delta, \theta, \alpha, \beta, \gamma\}$ corresponds to the EEG-band number. A five dimensional feature vector is formed by combining the energy features from δ, θ, α, β, and γ rhythms of the EEG signal. The least square SVM-based classifier is utilized in this investigation with the purpose to classify seizure and seizure-free classes, employing the energy features from the rhythms of EEG signal. In this work, we have normalized energy feature of each EEG instance based on the maximum of the energy values of all EEG instances [31]. The least square SVM technique has been been introduced for different biomedical applications such as detection of epileptic seizure [32], detection of breast cancer [33], and detection of various cardiac arrhythmia episodes [34]. Here, the feature matrix and the class labels are denoted as $\mathbf{X} = [\mathbf{x}_i]_{i=1}^m$ and $\mathbf{y} = [y_i]_{i=1}^m$, respectively. This feature matrix for this work mainly contains the five dimensional feature vectors with each feature vector as $\mathbf{x}_i \in R^p$ and $p = 5$. Similarly, the class label vector consists of the label of the i^{th} feature vector ($\mathbf{x}_i$) as $\mathbf{y} = [y_i]_{i=1}^m$, where $y_i = \{0, 1, 2\}$. Here, m corresponds to the total number of EEG signals ($m = 500$), and 0, 1, and 2 are the class label notations for normal, seizure-free, and seizure instances. The main task of the least square SVM technique is to evaluate the optimal weights and the bias by formulating a least square optimization problem, whose optimal formulation is given by [35]

$$\min \quad J(\mathbf{w}, b, \epsilon) = \frac{1}{2}\mathbf{w}^T\mathbf{w} + \frac{\eta}{2}\sum_{i=1}^{p}\gamma_i^2 \tag{9}$$

The equality constraint used in the above optimization problem is given as $y_i(\mathbf{w}^T f(\mathbf{x}_i) + b) = 1 - \eta_i$. Where the $\mathbf{w}$ and b stand for the q-dimensional weight vector and bias value, respectively. η_i refers to the slack variable used for the regularization purpose in the equation (9). The mapping such as the $f(\mathbf{x}_i)$ converts the input p-dimensional feature vector into a q-dimensional space. Taking the Lagrangian in (9), this becomes as

$$L(\mathbf{w}, b, \eta; \nu) = J(\mathbf{w}, b, \eta) - \sum_{i=1}^{m} \nu_i[y_i(\mathbf{w}^T f(\mathbf{x}_i) + b) - 1 + \eta_i] \tag{10}$$

The solution of the equation (10) will give rise to the corresponding Lagrange multipliers as $\nu = (\nu_1, \nu_2, ..., \nu_m)^T$ and the bias values. Thus, the output of the least square SVM classifier for a given test EEG feature vector $\mathbf{x}_t$ can be written as follows: [35]

$$f(\mathbf{x}_t) = sign[\sum_{i=1}^{m} \nu_i y_i K(\mathbf{x}, \mathbf{x}_i) + b] \tag{11}$$

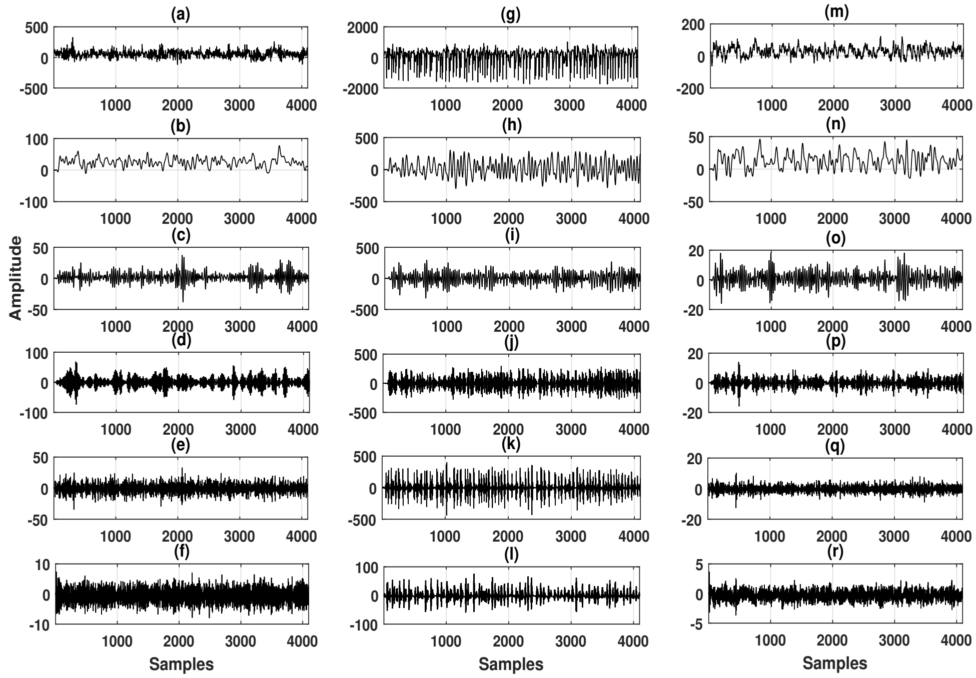

Fig. 4. (a) EEG signal for normal class. (b)-(f) The EEG rhythms obtained using proposed Taylor-Fourier filter bank implemented using O-splines for normal class. (g) EEG signal for seizure class. (h)-(l) The EEG rhythms obtained using proposed Taylor-Fourier filter bank implemented using O-splines for seizure class. (m) EEG signal for seizure-free class. (n)-(r) The EEG rhythms obtained using proposed Taylor-Fourier filter bank implemented using O-splines for seizure-free class.

TABLE II
STATISTICAL ANALYSIS OF THE TAYLOR-FOURIER BAND ENERGY FEATURES FOR NORMAL, SEIZURE-FREE AND SEIZURE CLASSES.

Features	Normal	Seizure	Seizure-free	p-value
$TFEBE_{\delta}$	0.0083 ± 0.0037	0.0038 ± 0.0036	0.0044 ± 0.0024	< 0.001
$TFEBE_{\theta}$	0.0022 ± 0.0014	0.0088 ± 0.0097	0.0016 ± 0.0007	< 0.001
$TFEBE_{\alpha}$	0.0009 ± 0.0007	0.0047 ± 0.0036	0.0036 ± 0.0027	< 0.001
$TFEBE_{\beta}$	0.0003 ± 0.0002	0.0023 ± 0.0020	0.0019 ± 0.0009	< 0.001
$TFEBE_{\gamma}$	0.00003 ± 0.00002	0.00018 ± 0.00010	0.00005 ± 0.00004	< 0.001

where the term $K(\mathbf{z}, \mathbf{z}_i)$ represents the kernel function. In this work, the radial basis function (RBF) kernel function is utilized for classification purposes. The training and test TF feature vectors of the EEG frames are chosen using hold-out, 10-fold and leave-one-out cross-validation approaches [36]. The performance of the least square-SVM with RBF classifier is evaluated using the accuracy, sensitivity, and specificity values [31]. In order to compare the performance of least square SVM, we have also used the K-nearest neighbor (KNN) [37], extreme learning machine (ELM) [38] and deep convolutional neural network (CNN) [39] models for the classification of normal, seizure-free and seizure classes.

III. Results and Discussion

As described in Fig. 1, we have exhibited the statistical analysis results of the proposed TFEBE features for normal, seizure-free and seizure classes, and the performance for both KNN and least square SVM classifiers. The statistical analysis is illustrated in terms of box-plots, evaluation of mean and standard deviation values of each feature for different classes, and student's t-test for statistical significance of the TFEBE features. Fig. 5 depicts the box-plots of TFEBE features for δ, θ, α, β, and γ-bands of the EEG signal. Moreover, we have also displayed the mean and the standard deviation values of the TFEBE features in Table II. From these results, we have observed that the mean values are different for normal, seizure, and seizure-free classes. From box-plot, it has also been noted that the median value and the quartiles (both upper and lower quartiles) are different for each class. The energy feature for the δ-rhythm has a lower mean value for seizure class as compared to normal and seizure-free classes. Moreover, for other bands (θ, α, β and γ-bands), the energy features have higher mean values for seizure class. The morphology of each EEG rhythm is different for seizure and normal classes, and during the seizure, the spikes are present in the EEG signal [40]. Due to this reason, the mean values of energy features for all EEG rhythms are different for normal, seizure and seizure-free classes. The statistical significance of the proposed TFEBE features is evaluated using the pair-wise test approach [41]. From the test result, it is observed that all TFEBE features have a p-value of less than 0.001 and, henceforth these features are significant for the classification of normal, seizure and seizure-free classes.

The classification performances of the KNN and least square-SVM classifiers are depicted in Tables III-V for hold-out, 10-fold, and leave-one-out cross-validation methodolo-

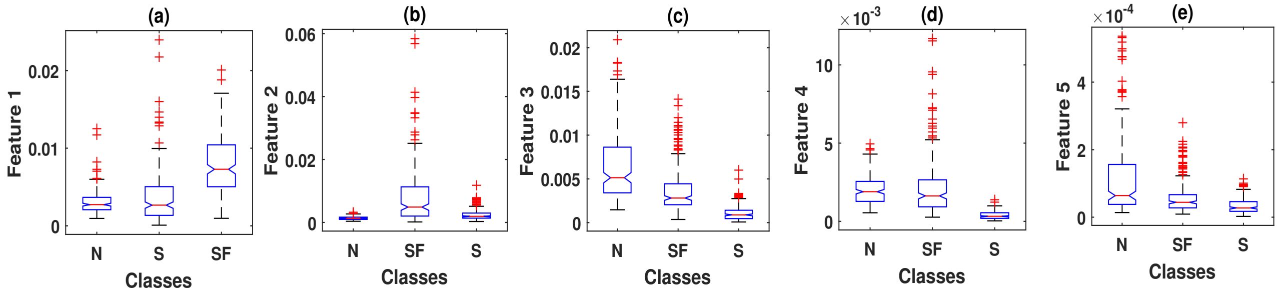

Fig. 5. Box-plots of every feature for the normal (N), seizure (S) and seizure-free (SF) classes. (a) Feature 1 (Energy of δ-rhythm); (b) feature 2 (Energy of θ-rhythm); (c) feature 3 (Energy of α-rhythm); (d) feature 4 (Energy of β-rhythm); and (e) feature 5 (Energy of γ-rhythm).

TABLE III

PERFORMANCE OF THE LEAST SQUARE SVM AND KNN CLASSIFIERS FOR TFEBE FEATURES AND HOLD-OUT CROSS-VALIDATION.

Feature selection	**Classifier**	**Experiment** % Training/Test	**Normal** $\mu \pm \sigma$	**Seizure-free** $\mu \pm \sigma$	**Seizure** $\mu \pm \sigma$	**Acc** $\mu \pm \sigma$	**Instance**
TF	KNN	70/30	91.49± 0.55	90.74± 1.67	76.40± 1.26	86.21 ± 0.57	3 sec
			93.68± 1.73	92.64 ± 1.37	73.44± 1.66	86.59 ±0.75	4 sec
			95.4± 0.89	92.4± 1.29	76.2 ± 3.58	88.00 ±1.02	5 sec
			96.93± 1.46	93.73±1.01	74.8±2.51	88.49 ±0.69	6 sec
			95.33±1.24	95.2±2.46	73.6±2.24	88.04±0.74	7 sec
			96.80± 1.64	96.20± 1.92	75.40±3.05	89.47 ±1.24	8 sec
			95.20± 1.48	95.40± 1.52	77.80± 4.55	89.47 ±1.61	9 sec
			97.20±1.30	92.60± 3.21	76.80±3.42	88.87±0.69	10 sec
TF	KNN	50/50	92.91 ± 1.42	91.49 ±0.79	72.97 ± 1.70	85.79 ± 0.56	3 sec
			92.48 ± 1.48	91.20 ±1.50	73.04 ± 3.88	85.57 ±1.83	4 sec
			93.90 ± 2.27	94.30 ±1.72	74.3 ± 3.05	87.50 ±1.69	5 sec
			95.33 ± 1.05	96.13 ±0.87	73.60 ± 2.24	88.36 ±0.80	6 sec
			96.40 ± 2.77	95.20 ±2.47	74.27 ± 1.53	88.62 ±0.55	7 sec
			97.20 ± 1.92	93.20 ±1.64	77.00 ± 2.00	89.13 ±0.77	8 sec
			94.80 ± 0.84	95.20 ±2.05	77.80 ± 3.70	89.27 ±0.86	9 sec
			96.80 ± 1.30	93.40 ±1.14	74.2 ± 4.87	88.13 ±1.12	10 sec
TF	Least square SVM with RBF	70/30	94.47 ± 0.99	93.61 ±2.25	86.67 ± 1.39	91.58 ± 0.75	3 sec
			95.99 ± 0.46	94.8 ±1.52	87.33 ± 1.56	92.71 ±0.91	4 sec
			96.32 ± 2.42	96.99 ±1.28	86.98 ± 2.73	93.43 ±0.72	5 sec
			98.67 ± 1.45	96.22 ±1.27	87.90 ± 0.83	94.28 ±0.66	6 sec
			96.87 ± 0.51	98.00 ±1.22	86.00 ± 1.27	93.62 ±0.57	7 sec
			98.00 ± 1.39	96.67 ±2.64	88.21 ± 2.36	94.31 ±1.27	8 sec
			96.67 ± 2.64	99.67 ±0.75	87.00 ± 3.21	94.44 ±1.04	9 sec
			97.22 ± 0.96	97.76 ±1.94	86.67 ± 2.89	93.88 ±0.02	10 sec
TF	Least square SVM with RBF	50/50	95.48 ± 0.96	94.11 ± 1.29	86.13 ± 2.67	91.91 ± 0.51	3 sec
			96.23 ± 2.10	95.66 ± 1.40	85.57 ± 3.92	92.48 ± 0.97	4 sec
			96.49 ± 0.80	95.79 ± 1.17	86.56 ± 0.73	92.95 ± 0.30	5 sec
			96.93 ± 0.76	96.00 ± 1.83	83.82 ± 2.00	92.26 ± 0.85	6 sec
			96.93 ± 1.80	96.11 ± 2.20	84.60 ± 2.21	92.55 ± 0.72	7 sec
			95.18 ± 1.65	96.40 ± 2.30	81.80 ± 2.49	91.12 ± 0.90	8 sec
			96.40 ± 1.34	96.40 ± 1.95	90.35 ± 1.09	94.39 ± 0.96	9 sec
			97.40 ± 1.52	96.00 ± 1.73	88.93 ± 2.67	94.12 ± 0.78	10 sec

gies, respectively. It is observed that for hold-out cross-validation with 70% of EEG instances as training and the remaining 30% instances as testing, the performance of both classifiers is high. Moreover, the least-square SVM-based classifier has shown higher average overall accuracy as compared to the KNN for each cross-validation method. We have also evaluated the performance of both classifiers by varying the EEG segment duration, as presents in Table IV. It is observed that both KNN and least square SVM classifiers have the highest overall accuracy values for the TFEBE features of the 9 sec EEG segment. Therefore, the 9-sec duration is found as the optimal window length for the Taylor-Fourier based filter-bank implemented with O-splines for the analysis of the EEG signal. For 10-fold cross-validation, the overall accuracy of

TABLE IV
PERFORMANCE OF THE LEAST SQUARE SVM AND KNN CLASSIFIERS FOR TFEBE FEATURES AND 10-FOLD CROSS-VALIDATION.

Classifier	Folds	Normal-IA (%)	Seizure-free-IA (%)	Seizure-IA (%)	OA (%)
KNN	1	100.00	93.33	76.67	90.00
	2	96.67	96.67	73.33	88.89
	3	96.67	93.33	76.67	88.89
	4	96.67	93.33	80.00	90.00
	5	93.33	96.67	86.67	92.22
	6	93.33	96.67	76.67	88.89
	7	100.00	93.33	63.33	85.56
	8	96.67	90.00	90.00	92.22
	9	100.00	90.00	73.33	87.78
	10	93.33	96.67	80.00	90.00
$\mu \pm \sigma$		96.67 ± 2.72	94.00 ±2.62	77.67 ±7.38	89.44 ±1.98
Least square SVM	1	100.00	96..67	86.67	94.44
	2	100.00	93.33	96.67	96.67
	3	93.33	96.67	76.67	88.89
	4	96.67	100.00	93.33	96.67
	5	100.00	100.00	90.00	96.67
	6	100.00	90.00	90.00	93.33
	7	100.00	100.00	90.00	96.67
	8	93.33	96.67	93.33	94.44
	9	100.00	93.33	96.67	96.67
	10	100.00	93.33	90.00	94.44
$\mu \pm \sigma$		98.33 ± 2.83	96.00 ±3.44	90.33 ±5.76	94.88 ±2.47

TABLE V
PERFORMANCE OF THE LEAST SQUARE SVM AND KNN CLASSIFIERS FOR TFEBE FEATURES AND LEAVE-ONE-OUT CROSS-VALIDATION.

Classifier	Accuracy (%)
KNN	87.70
Least square SVM	91.00

the least square SVM classifier is higher for normal, seizure and seizure-free classes as compared to the KNN classifier. Moreover, for leave-one-out cross-validation, the least square SVM classifier has an accuracy value of 91.00%. The least-square SVM classifier has the highest overall accuracy value for all three cross-validation approaches. Moreover, we have compared the performance of the least square SVM classifier with ELM [38] and deep CNN [39] classifiers for the epileptic seizure detection. The hold-out cross-validation with 70% EEG instances as training and 30% EEG instances as testing are considered for both deep CNN and ELM classifiers. The RBF based activation function, the number of hidden neurons as 100, and the regularization parameter as 0.9 are considered for the ELM classifier using TFEBE features of the EEG signal. Similarly, for deep CNN, we have considered the architecture as [input layer, convolution layer 1-pooling layer 1- convolution (Conv) layer 2- pooling layer 2-Conv layer 3-pooling layer 3- Conv layer 4-pooling layer 4-Conv layer 5-pooling layer 5- fully connected layer 1-fully connected layer 2-fully connected layer 3-output layer]. The number of filters and filter sizes in the Conv layer 1, Conv layer 2, Conv layer 3, Conv layer 4, and Conv layer 5 are (4, 6), (4, 5), (10, 4), (10, 4), (10, 4), and (15, 4), respectively. The stride for each Conv layer is considered as 1. Moreover, for each pooling layer, we have considered average pooling, pooling factor as 2, and stride as 2, respectively. The number of neurons in the second and third fully connected layers is 50 and 20, respectively. The input to the deep CNN classifier for an EEG instance is represented as (4096×5). Where 4096 is the number of samples and 5 is the number of rhythms of the EEG signal. The deep CNN architecture can be termed as the multi rhythm deep CNN for the classification of normal, seizure-free and seizure EEG signals. The individual accuracy values for normal, seizure-free and seizure classes, and the overall accuracy value for ELM and deep CNN classifiers are shown in Table VI. It has been observed that the performance of ELM and deep CNN classifiers are less than the least square SVM classifier for the classification of seizure, seizure-free and normal EEG signals. The performance of the proposed method is also compared with the energy features extracted from the EEG rhythm specific Hamming window-based finite impulse response (FIR) bandpass filters [49]. The order for each FIR filter is selected as 100. The average overall accuracy value is obtained as 92.99% using the least square SVM classifier coupled with the energy features extracted from the rhythm specific FIR filters and 10-fold cross-validation based selection of EEG instances. It is observed that the least square SVM classifier has higher overall accuracy value using the energy features from the subband signals of the proposed filter-bank as compared to the EEG rhythm specific FIR filters. This shows the effectiveness of the Taylor-Fourier filter-bank implemented using O-splines for extracting EEG rhythm specific subband signals for the detection of epileptic seizures.

In this study, we have compared the performance of the least square SVM classifier with existing approaches for the classification of normal, epileptic seizure, and seizure-free classes from the EEG signal. Comparisons are illustrated in Table VII. Ghosh-Dastidar and Adeli [42] have designed the spiking neural network to classify seizure, seizure-free and normal classes from the EEG signal. They have obtained an overall accuracy value of 92.50%. Moreover, in another study, Chua et al. [43] have extracted the higher-order spectral features from the EEG signal. The higher-order spectral features and SVM classifier are used for the classification of normal, seizure and seizure-free classes with an overall accuracy value of 93.11%. Similarly, Acharya et al. [44] have used the deep convolutional neural network (CNN) for the classification of normal, seizure-free, and seizure classes from the EEG signals. The deep CNN classifier has an overall accuracy value of 88.70%. The proposed method has higher performance as compared to the reported works in [42] [43] [44]. Moreover, Li et al. [47] have extracted various entropy features from EEG signal. They have used the SVM classifier for the classification of seizure-free and seizure classes with an overall accuracy value of 93%. Similarly, Amarantidis and Abasolo [48] have extracted features from the EEG signal using different entropy measures and used k-nearest neighbor classifier for the detection of seizure. An overall accuracy value of 73.50% has been reported. Martis et al. [46] have evaluated energy, peaks, and entropy from the spectrum of

TABLE VI
PERFORMANCE OF THE ELM AND DEEP CNN CLASSIFIERS FOR HOLD-OUT CROSS-VALIDATION.

Classifier	Classifier Input	Normal-IA (%)	Seizure-free-IA (%)	Seizure-IA (%)	OA (%)
ELM	TFEBE features	82.99 ± 2.71	93.28 ± 2.95	50.09 ± 2.85	75.18 ± 1.46
Deep CNN	Subband signals matrix	70.83 ± 1.66	72.49 ± 5.69	78.33 ± 3.33	73.88 ± 2.31

TABLE VII
COMPARISON WITH EXISTING APPROACHES FOR THE CLASSIFICATION OF NORMAL, SEIZURE AND SEIZURE-FREE CLASSES.

Feature Extraction Methods	Classifier Used	OA(%)
Direct EEG Signal as input [42]	Spiking Neural Network	92.5%
Higher Order Spectral Features [43]	SVM	93.11%
Convolution and Pooling Layers [44]	CNN	88.70%
Principal components from wavelet coefficients of EEG [45]	Fuzzy inference system	96.70%
Spectral features from each IMF of EEG [46]	CART	95.33%
Entropy features from EEG signal [47]	Quadratic discriminant classifier	93.00%
Different entropies extracted from EEG signal [48]	k-nearest neighbour classifier	73.50%
TFEBE Features (Proposed work)	Least-square SVM	94.88%

each intrinsic mode function (IMF) of the EEG signal. They have used classification and regression tree (CART) model to classify the normal, inter-ictal and ictal classes, and reported an average accuracy of 95.33%. Similarly, Acharya et al. [45] have used wavelet packet decomposition (WPD) and principal component analysis (PCA) for extracting features from the EEG signal. They have considered a fuzzy inference system-based classifier obtaining an overall accuracy value of 96.7%. The proposed method has less overall accuracy value as compared to the EMD and wavelet packet-based approaches. The existing methods used wavelet transform which further requires basis functions and the number of decomposition levels for EEG signal analysis [45]. The proposed method is simple as compared to wavelet and EMD based approaches as it uses O-splines to design the EEG rhythm specific filter-bank. The computational complexity for the design of the Taylor-Fourier filter-bank with O-splines is evaluated as follows. According to the signal model used by the DTFT in (3) and its traditional implementation presented in [29], [50], the highest computational burden is required by inverting the matrix Φ_K. This has been employed into the analysis equation $\hat{\xi}_K = \Phi_K^{\dagger} z_k$, requiring $(CN)^2$ products; whereas from (5) only $C(N+1)$ products are needed, this means that the matrix inversion process is not required anymore. Thus, the total computational complexity required for the straightforward implementation of the O-splines for extracting 5 different rhythms is given by $5CN$, recalling that $C = K+1$. In [51], the computational complexity of the EMD algorithm has been evaluated as $41S.N \log_2(N)$. where S is the number of sifting operations and 'N' is the length of the signal. Similarly, the computational complexity of WPD is $2^{(L+1)} N \log_2(N)$ [52]. where L is the number of decomposition levels. It is observed that the proposed method has less computational complexity as compared to EMD and WPD approaches. Instead of extracting energy features, the EEG rhythms obtained using the proposed approach can be used as the input to various deep neural network [44] [53] for the classification of seizure and non-seizure classes.

IV. CONCLUSION

In this paper, an approach based on the EEG-rhythm specific Taylor-Fourier filter-bank implemented using O-splines has been proposed for the classification of seizure and non-seizure classes. The TFEBE features have been extracted from the EEG-rhythms and the classifiers such as the KNN and least square SVM are used for the classification. The classification results have been evaluated for all three cross-validation techniques based EEG instance selection for the classification of normal, seizure and non-seizure classes. For leave one out cross-validation, an average accuracy value of 91% has been reported using the least square SVM classifier. The method has shown better performance as compared to the deep CNN for the classification of seizure, seizure-free and normal classes from the EEG signal.

V. ACKNOWLEDGEMENT

The authors are thankful to Mr. Daksh Maheshwari for the help in the coding part of CNN with hold-out cross-validation approach.

REFERENCES

[1] C. Franchi, G. Giussani, P. Messina, M. Montesano, S. Romi, A. Nobili, I. Fortino, A. Bortolotti, L. Merlino, E. Beghi *et al.*, "Validation of healthcare administrative data for the diagnosis of epilepsy," *J Epidemiol Community Health*, vol. 67, no. 12, pp. 1019–1024, 2013.

[2] R. S. Fisher, W. Van Emde Boas, W. Blume, C. Elger, P. Genton, P. Lee, and J. Engel Jr, "Response: definitions proposed by the international league against epilepsy (ilae) and the international bureau for epilepsy (ibe)," *Epilepsia*, vol. 46, no. 10, pp. 1701–1702, 2005.

[3] J. Saini and M. Dutta, "An extensive review on development of eeg-based computer-aided diagnosis systems for epilepsy detection," *Network: Computation in Neural Systems*, vol. 28, no. 1, pp. 1–27, 2017.

[4] U. R. Acharya, S. V. Sree, and J. S. Suri, "Automatic detection of epileptic eeg signals using higher order cumulant features," *International journal of neural systems*, vol. 21, no. 05, pp. 403–414, 2011.

[5] C. Mahjoub, R. L. B. Jeannès, T. Lajnef, and A. Kachouri, "Epileptic seizure detection on eeg signals using machine learning techniques and advanced preprocessing methods," *Biomedical Engineering/Biomedizinische Technik*, 2019.

[6] K. Fu, J. Qu, Y. Chai, and T. Zou, "Hilbert marginal spectrum analysis for automatic seizure detection in eeg signals," *Biomedical Signal Processing and Control*, vol. 18, pp. 179–185, 2015.

[7] M. Srirangan, R. K. Tripathy, and R. B. Pachori, "Time-frequency domain deep convolutional neural network for the classification of focal and non-focal eeg signals," *IEEE Sensors Journal*, pp. 1–1, 2019.

[8] M. Peker, B. Sen, and D. Delen, "A novel method for automated diagnosis of epilepsy using complex-valued classifiers," *IEEE journal of biomedical and health informatics*, vol. 20, no. 1, pp. 108–118, 2015.

[9] V. Gupta and R. Pachori, "Epileptic seizure identification using entropy of fbse based eeg rhythms," *Biomedical Signal Processing and Control*, 05 2019.
[10] A. Bhattacharyya, R. Pachori, A. Upadhyay, and U. Acharya, "Tunable-q wavelet transform based multiscale entropy measure for automated classification of epileptic eeg signals," *Applied Sciences*, vol. 7, no. 4, p. 385, 2017.
[11] M. Sharma, R. B. Pachori, and U. R. Acharya, "A new approach to characterize epileptic seizures using analytic time-frequency flexible wavelet transform and fractal dimension," *Pattern Recognition Letters*, vol. 94, pp. 172–179, 2017.
[12] R. R. Sharma and R. B. Pachori, "Time–frequency representation using ievdhm–ht with application to classification of epileptic eeg signals," *IET Science, Measurement & Technology*, vol. 12, no. 1, pp. 72–82, 2017.
[13] V. Gupta, A. Bhattacharyya, and R. B. Pachori, "Automated identification of epileptic seizures from eeg signals using fbse-ewt method," *Biomedical Signal Processing-Advances in Theory, Algorithms and Applications, Springer*, 2019.
[14] Y. R. Aldana, B. Hunyadi, E. J. M. Reyes, V. R. Rodríguez, and S. Van Huffel, "Nonconvulsive epileptic seizure detection in scalp eeg using multiway data analysis," *IEEE Journal of Biomedical and Health Informatics*, vol. 23, no. 2, pp. 660–671, 2018.
[15] Y. Li, W. Cui, M. Luo, K. Li, and L. Wang, "Epileptic seizure detection based on time-frequency images of eeg signals using gaussian mixture model and gray level co-occurrence matrix features," *International journal of neural systems*, vol. 28, no. 07, p. 1850003, 2018.
[16] D. Bhati, M. Sharma, R. B. Pachori, and V. M. Gadre, "Time–frequency localized three-band biorthogonal wavelet filter bank using semidefinite relaxation and nonlinear least squares with epileptic seizure eeg signal classification," *Digital Signal Processing*, vol. 62, pp. 259–273, 2017.
[17] R. Sharma and R. B. Pachori, "Classification of epileptic seizures in eeg signals based on phase space representation of intrinsic mode functions," *Expert Systems with Applications*, vol. 42, no. 3, pp. 1106–1117, 2015.
[18] V. Joshi, R. B. Pachori, and A. Vijesh, "Classification of ictal and seizure-free eeg signals using fractional linear prediction," *Biomedical Signal Processing and Control*, vol. 9, pp. 1–5, 2014.
[19] P. Swami, T. K. Gandhi, B. K. Panigrahi, M. Tripathi, and S. Anand, "A novel robust diagnostic model to detect seizures in electroencephalography," *Expert Systems with Applications*, vol. 56, pp. 116–130, 2016.
[20] A. K. Jaiswal and H. Banka, "Local pattern transformation based feature extraction techniques for classification of epileptic eeg signals," *Biomedical Signal Processing and Control*, vol. 34, pp. 81–92, 2017.
[21] Y. Li, X.-D. Wang, M.-L. Luo, K. Li, X.-F. Yang, and Q. Guo, "Epileptic seizure classification of eegs using time–frequency analysis based multiscale radial basis functions," *IEEE journal of biomedical and health informatics*, vol. 22, no. 2, pp. 386–397, 2017.
[22] A. T. Tzallas, M. G. Tsipouras, and D. I. Fotiadis, "Automatic seizure detection based on time-frequency analysis and artificial neural networks," *Computational Intelligence and Neuroscience*, vol. 2007, 2007.
[23] K. Fu, J. Qu, Y. Chai, and Y. Dong, "Classification of seizure based on the time-frequency image of eeg signals using hht and svm," *Biomedical Signal Processing and Control*, vol. 13, pp. 15–22, 2014.
[24] Y. Kumar, M. Dewal, and R. Anand, "Epileptic seizure detection using dwt based fuzzy approximate entropy and support vector machine," *Neurocomputing*, vol. 133, pp. 271–279, 2014.
[25] J. A. de la O Serna, "Analyzing power oscillating signals with the O-splines of the discrete taylorfourier transform," vol. 33, no. 6, pp. 7087–7095, Nov 2018.
[26] R. K. Tripathy, A. Zamora-Mendez, S. de la O, A. José, M. R. A. Paternina, J. G. Arrieta, and G. R. Naik, "Detection of life threatening ventricular arrhythmia using digital taylor fourier transform," *Frontiers in physiology*, vol. 9, p. 722, 2018.
[27] R. G. Andrzejak, K. Lehnertz, F. Mormann, C. Rieke, P. David, and C. E. Elger, "Indications of nonlinear deterministic and finite-dimensional structures in time series of brain electrical activity: Dependence on recording region and brain state," *Physical Review E*, vol. 64, no. 6, p. 061907, 2001.
[28] P. Sircar, R. B. Pachori, and R. Kumar, "Analysis of rhythms of eeg signals using orthogonal polynomial approximation," in *Proceedings of the 2009 international conference on hybrid information technology*. ACM, 2009, pp. 176–180.
[29] J. A. de la O Serna, "Taylor–fourier analysis of blood pressure oscillometric waveforms," *IEEE Transactions on Instrumentation and Measurement*, vol. 62, no. 9, pp. 2511–2518, 2013.
[30] P. Olejniczak, "Neurophysiologic basis of eeg," *Journal of clinical neurophysiology*, vol. 23, no. 3, pp. 186–189, 2006.
[31] R. Tripathy, L. Sharma, and S. Dandapat, "Detection of shockable ventricular arrhythmia using variational mode decomposition," *Journal of medical systems*, vol. 40, no. 4, p. 79, 2016.
[32] V. Bajaj and R. B. Pachori, "Classification of seizure and nonseizure eeg signals using empirical mode decomposition," *IEEE Transactions on Information Technology in Biomedicine*, vol. 16, no. 6, pp. 1135–1142, 2012.
[33] R. K. Tripathy, S. Mahanta, and S. Paul, "Artificial intelligence-based classification of breast cancer using cellular images," *RSC Advances*, vol. 4, no. 18, pp. 9349–9355, 2014.
[34] K. Polat, B. Akdemir, and S. Güneş, "Computer aided diagnosis of ecg data on the least square support vector machine," *Digital Signal Processing*, vol. 18, no. 1, pp. 25–32, 2008.
[35] J. A. Suykens and J. Vandewalle, "Least squares support vector machine classifiers," *Neural processing letters*, vol. 9, no. 3, pp. 293–300, 1999.
[36] R. J. Martis, U. R. Acharya, C. M. Lim, and J. S. Suri, "Characterization of ecg beats from cardiac arrhythmia using discrete cosine transform in pca framework," *Knowledge-Based Systems*, vol. 45, pp. 76–82, 2013.
[37] P. Cunningham and S. J. Delany, "k-nearest neighbour classifiers," *Multiple Classifier Systems*, vol. 34, no. 8, pp. 1–17, 2007.
[38] G.-B. Huang, H. Zhou, X. Ding, and R. Zhang, "Extreme learning machine for regression and multiclass classification," *IEEE Transactions on Systems, Man, and Cybernetics, Part B (Cybernetics)*, vol. 42, no. 2, pp. 513–529, 2011.
[39] H.-C. Shin, H. R. Roth, M. Gao, L. Lu, Z. Xu, I. Nogues, J. Yao, D. Mollura, and R. M. Summers, "Deep convolutional neural networks for computer-aided detection: Cnn architectures, dataset characteristics and transfer learning," *IEEE transactions on medical imaging*, vol. 35, no. 5, pp. 1285–1298, 2016.
[40] S. Smith, "Eeg in the diagnosis, classification, and management of patients with epilepsy," *Journal of Neurology, Neurosurgery & Psychiatry*, vol. 76, no. suppl 2, pp. ii2–ii7, 2005.
[41] W. E. Martin and K. D. Bridgmon, *Quantitative and statistical research methods: From hypothesis to results*. John Wiley & Sons, 2012, vol. 42.
[42] S. Ghosh-Dastidar and H. Adeli, "Improved spiking neural networks for eeg classification and epilepsy and seizure detection," *Integrated Computer-Aided Engineering*, vol. 14, no. 3, pp. 187–212, 2007.
[43] K. C. Chua, V. Chandran, U. R. Acharya, and C. M. Lim, "Application of higher order spectra to identify epileptic eeg," *Journal of medical systems*, vol. 35, no. 6, pp. 1563–1571, 2011.
[44] U. R. Acharya, S. L. Oh, Y. Hagiwara, J. H. Tan, and H. Adeli, "Deep convolutional neural network for the automated detection and diagnosis of seizure using eeg signals," *Computers in biology and medicine*, vol. 100, pp. 270–278, 2018.
[45] U. R. Acharya, S. V. Sree, A. P. C. Alvin, and J. S. Suri, "Use of principal component analysis for automatic classification of epileptic eeg activities in wavelet framework," *Expert Systems with Applications*, vol. 39, no. 10, pp. 9072–9078, 2012.
[46] R. J. Martis, U. R. Acharya, J. H. Tan, A. Petznick, R. Yanti, C. K. Chua, E. K. Ng, and L. Tong, "Application of empirical mode decomposition (emd) for automated detection of epilepsy using eeg signals," *International journal of neural systems*, vol. 22, no. 06, p. 1250027, 2012.
[47] P. Li, C. Karmakar, J. Yearwood, S. Venkatesh, M. Palaniswami, and C. Liu, "Detection of epileptic seizure based on entropy analysis of short-term eeg," *PloS one*, vol. 13, no. 3, p. e0193691, 2018.
[48] L. C. Amarantidis and D. Abásolo, "Interpretation of entropy algorithms in the context of biomedical signal analysis and their application to eeg analysis in epilepsy," *Entropy*, vol. 21, no. 9, p. 840, 2019.
[49] J. G. Proakis, *Digital signal processing: principles algorithms and applications*. Pearson Education India, 2001.
[50] M. R. A. Paternina, J. M. Ramirez, and A. Z. Méndez, "Real-time implementation of the digital taylor–fourier transform for identifying low frequency oscillations," *Electric Power Systems Research*, vol. 140, pp. 846–853, 2016.
[51] Y.-H. Wang, C.-H. Yeh, H.-W. V. Young, K. Hu, and M.-T. Lo, "On the computational complexity of the empirical mode decomposition algorithm," *Physica A: Statistical Mechanics and its Applications*, vol. 400, pp. 159–167, 2014.
[52] M. Feil and A. Uhl, "Wavelet packet decomposition and best basis selection on massively parallel simd arrays," in *Proceedings of the International Conference Wavelets and Multiscale Methods(IWC98), Tangier*. Citeseer, 1998.
[53] O. Faust, Y. Hagiwara, T. J. Hong, O. S. Lih, and U. R. Acharya, "Deep learning for healthcare applications based on physiological signals: A review," *Computer methods and programs in biomedicine*, vol. 161, pp. 1–13, 2018.

José Antonio de la O Serna (SM'03) received his Ph.D. degree from Telecom ParisTech, France, in 1982. In 1987 he joined the Ph.D. program in electrical engineering at the Autonomous University of Nuevo Len (UANL), where he was a Member of the Doctoral Committee. Currently he is a research professor at the UANL, Monterrey, Mexico. He was also a professor at Monterrey Institute of Technology from 1982 to 1986. From 1988 to 1993, he was with the Electrical Department at the Polytechnic School in Yaound, Cameroon. Mr. de la O Serna is a Member of the Mexican Research System.

Mario R. Arrieta Paternina (M' 11) Mario Arrieta-Paternina holds a B.S. and M.Sc. in Electrical Engineering from National University of Colombia, in 2007 and 2009, respectively. In 2017, he obtained his Ph.D. degree in electrical engineering from CINVESTAV. He joined the Department of Electrical Engineering at University of Mexico, in 2017. He was a visiting scholar at Rensselaer Polytechnic Institute in 2016. His areas of interest include dynamic equivalents, coherency, modal identification, and model reduction of power systems. He is a Member of IEEE and the Power Energy IEEE Society from 2011.

Alejandro Zamora-Méndez (M' 11) Alejandro Zamora obtained his B.S. and M.Sc. in Electrical Engineering from Universidad Michoacana de San Nicolas de Hidalgo (UMSNH), Morelia, Mexico, in 2005 and 2008, respectively. He joined the Electrical Engineering Faculty, UMSNH, in 2008, where he is a full-time Professor. He received the Ph.D. degree from CINVESTAV-Guadalajara in 2016. His areas of interest include oscillation monitoring, signal processing, coherency, modal identification, and power system dynamics and control.

Rajesh Kumar Tripathy received the B.Tech degree in Electronics and Telecommunication Engineering from the Biju Patnaik University of Technology (BPUT), Odisha, India, in 2009, and the M.Tech degree in Biomedical Engineering from the National Institute of Technology (NIT) Rourkela, Rourkela, India, in 2013, and the Ph.D. degree in Biomedical signal processing under Electronics and Electrical Engineering (EEE) department from the Indian Institute of Technology (IIT) Guwahati, Guwahati, India in 2017. He worked as an Assistant Professor at faculty of engineering and technology (FET), Siksha 'O' Anusandhan Deemed to be University from march, 2017 to June 2018. From July 2018, he is working as an Assistant Professor in the Department of Electrical and Electronics Engineering (EEE), Birla Institute of Technology and Science (BITS), Pilani, Hyderabad Campus. His research interests are Digital Signal Processing for biomedical applications, Sensor Data Processing, Machine Learning, Medical Image Processing and Internet of Things (IOT) for Healthcare. He has published research papers in reputed international journals and conferences. He has served as a reviewer for more than 15 scientific journals and served as a technical program committee (TPC) member in various national and international conferences.

Ram Bilas Pachori received the B.E. degree with honours in Electronics and Communication Engineering from Rajiv Gandhi Technological University, Bhopal, India in 2001, the M.Tech. and Ph.D. degrees in Electrical Engineering from Indian Institute of Technology (IIT) Kanpur, Kanpur, India in 2003 and 2008, respectively. He worked as a Postdoctoral Fellow at Charles Delaunay Institute, University of Technology of Troyes, Troyes, France during 2007-2008. He served as an Assistant Professor at Communication Research Center, International Institute of Information Technology, Hyderabad, India during 2008-2009. He served as an Assistant Professor at Discipline of Electrical Engineering, IIT Indore, Indore, India during 2009-2013. He worked as an Associate Professor at Discipline of Electrical Engineering, IIT Indore, Indore, India during 2013-2017 where presently he has been working as a Professor since 2017. He is also an Associated Faculty with Discipline of Biosciences & Biomedical Engineering at IIT Indore. He was a Visiting Professor at School of Medicine, Faculty of Health and Medical Sciences, TaylorŁs University, Subang Jaya, Malaysia during 2018- 2019. He worked as a Visiting Scholar at Intelligent Systems Research Center, Ulster University, Northern Ireland, UK during December 2014. He is an Associate Editor of Electronics Letters, Biomedical Signal Processing and Control journal and an Editor of IETE Technical Review journal. He is a senior member of IEEE and a Fellow of IETE. He has more than 185 publications which include journal papers, conference papers, books, and book chapters. His publications have around 5500 citations, h index of 40, and i10 index of 94 (Google Scholar, February 2020). He has served on review boards for around 100 scientific journals and served for scientific committees of various national and international conferences. His research interests are in the areas of biomedical signal processing, non-stationary signal processing, speech signal processing, signal processing for communications, computer-aided medical diagnosis, and signal processing for mechanical systems.